Experimental and numerical analysis of a CFRP strengthened steel-concrete composite beam

Yazar(lar) (Author(s)): Emre ERCAN[1], Bengi ARISOY[1], Emin HÖKELEKLİ[2]

ORCID[1]: 0000-0001-9325-8534

ORCID[2]: 0000-0002-2785-0609

ORCID[3]: 0000-0003-0548-5214

Experimental and Numerical Analysis of a CFRP Strengthened Steel-Concrete Composite Beam

Emre ERCAN[1*], Bengi ARISOY[1], Emin HÖKELEKLİ[2]

[1] Faculty of Engineering, Civil Engineering Department, Ege University, İzmir, Turkey
[2] Faculty of Engineering, Civil Engineering Department, Bartın University, Bartın, Turkey

ABSTRACT

In this study, experimental and nonlinear finite element analysis of strengthened steel-concrete composite beams is presented. A steel-concrete composite beam is produced by using a steel beam and concrete slab bonded each other with shear connectors. Strengthening is applied by Carbon Fiber Reinforced Polymers (CFRP) sheets to the lower flange of the steel beam. Three samples are prepared, one of them is considered as a reference sample, the other two are strengthened by CFRP sheets with different number of layers. In experimental study, steel-concrete composite beams were tested by 4-point bending test with cyclic loading. During the test, load, deflection, and strain values are measured. Then 3D finite element models of the steel-concrete composite beams are prepared using tetrahedral elements. Finite element analysis is performed by using ATENA nonlinear analysis program. The results of experiments and finite element analysis are compared. Results indicated that the strengthened steel-concrete composite beams have larger moment capacity, lower deflection that the steel-concrete composite beam sample. Some evaluations are made on especially in terms of strength, applicability, stiffness and energy consumption about the steel-concrete composite beams with CFRP. Experimental results are found similar to the results obtained by nonlinear finite element method.

Keywords: CFRP, strengthened steel-composite beam, 4-point loading test, FEM High speed processing of ferrous or non-

1. INTRODUCTION

The bearing system mentioned that produced as a result of merging reinforced concrete slabs and the steel beams with shear elements (shear connectors) is called a steel-concrete composite beam (Figure 1). These systems are more economical than steel beams that bear alone the concrete slab that sits freely on them. This is because in steel-concrete composite beams the tension component of the force pair originating from bending is carried by the steel profile, and the compressive component is carried only by the concrete slab or jointly with upper portion of the steel beam. Therefore, a steel profile that is weak against buckling is relieved entirely or to a large extent from carrying the compressive component of bending.
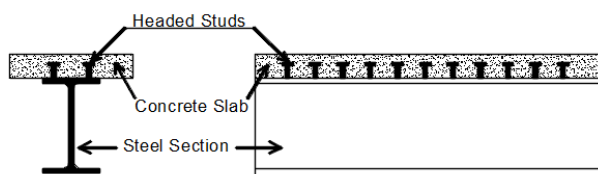

Figure1. Typical steel-concrete composite beam [2]

Two types of steel-concrete composite beams can be fabricated, fully and partially; a fully-composite beam

has a sufficient number of shear connectors (headed studs) that prevent the slip between the concrete and steel

Corresponding Author (Sorumlu yazar)
e-posta : emre.ercan@ege.edu.tr

beam after concrete crushing and steel beam yielding. In a partially steel-concrete composite beam, shear connectors fail before the concrete crushing under compression and the slip between the concrete and steel beam would occur [1,2]. The performance of the steel-concrete composite beams is depending on the capacity of the shear members between the reinforced concrete slab and the steel beam [3].

Steel-concrete composite beams have been used as main structural members in flexure for bridges and building constructions. The maximum load and moment capacity of steel-concrete composite beams under bending moment can be improved by applying Carbon Fiber Reinforced Polymers (CFRP) to lower flange of the steel beam. Strengthening of steel-concrete composite beams include: increasing the load-carrying capacity and the resistance to withstand underestimated loads; preventing failure due to inadequate detailing; recovering lost load carrying capacity due to degradation caused by aging or corrosion [4-7]. The problem in strengthened with CFRP is de-bonding of CFRP from strengthened members. De-bonding takes place in high stress concentration regions due to cracks. There are two main de-bonding failure modes between steel and CFRP, intermediate de-bonding due to yielding of steel and, plate end de-bonding [8]. In the literature, there are many studies associated with steel-concrete composite beams. Studies are typically based on strengthening concrete and steel with a variety of materials. Some of the studies are summarized below:

Teng et al [9], investigated strengthened steel-concrete composite beams with CFRP under bending experimentally and numerically. In the study they exhibited increase in moment capacity and the location

of de-bonding between CFRP sheets and steel under heavy loads. El-Shihy et al. [10], conducted an experiment and a nonlinear FEM analysis on the behavior of steel-concrete composite beams strengthened in hogging moment region with CFRP sheets. Experimental results showed strengthening steel-concrete composite beams with concrete slab with CFRP sheets with one and two layers increased the load carrying capacity of the beam by 15% and 21%, respectively. The stress at the edge of the CFRP sheets are found higher than those at its center and the difference increases as the CFRP sheet width increases due to a shear lag effect in the concrete substrate. They conduct nonlinear FEM analyses on ABAQUS and the FEM results of capacity load-deflection curves were calculated higher than experimental results. Pecce et.al. [11], investigated the rotational capacity of steel-concrete composite beams, for seismic design of composite frames and the effects of various parameters on the available plastic rotation. Lin et. al. [12], described the fatigue behavior of steel-concrete composite beams under negative bending moment. They performed fatigue tests with repeated load limited to stabilized cracking and initial cracking on two steel-concrete composite beams. They observed that when the repeated load was chosen to the initial cracking load, the fatigue test had very small influence on stiffness of the steel-concrete composite beam. However, when the repeated load was chosen equivalent to the stabilized cracking load, a number of residual cracks occurred in the initial static test and the beam lost stiffness as the load cycles increase. If the repeated load had been chosen larger than the initial cracking load, stiffness and ultimate load carrying capacity of beam would be decreased. Sallam et. al. [8], investigate the effect of pre-intermediate separation on the flexural behavior of strengthened steel-concrete composite beams retrofitted by CFRP and showed the intermediate de-bonding started growing after yielding of the steel flange. Değerli [13] investigated shear members of the steel-concrete composite beams. He used bolts as shear connectors and investigated the composite working status, the scraping status of the slab and the effect of placement of bolts at different intervals on the transportation strength and crack formation experimentally. It was confirmed that the bolts are very good slip coupling elements. In the study conducted by Ağcakoca and Aktaş [14], it was aimed to determine the necessary CFRP amount to ensure designed behavior in reinforced steel-concrete composite beams. They obtained reinforced beams by applying a High Modulus-CFRP strip to the bottom flange of the steel beam that was forming a composite profile and the beam was subjected to a 4-point loading test. The collapse occurred with the rupture of HM-CFRP strips. In the study conducted by Özyılmaz [15] the effect of CFRP sheets on steel-concrete composite beams studied experimentally under 4-point loadings tests.

In this study experimental and nonlinear finite element analysis of strengthened steel-concrete composite beams are presented. In experimental study, steel-concrete composite beams were tested by 4-point bending test with cyclic loading. Load, deflection, and strain values are measured. Then 3D finite element models of the steel-concrete composite beams are prepared and analyzed. The experimental and analytical results were compared. Significant feature of the study is to exhibit efficiency and applicability of strengthening.

2. EXPERIMENTAL STUDY

The steel-concrete composite beams with a length of 3m and a span of 2.70 m are tested in 4-point bending test. The beam has two parts steel beam and concrete slab. These two parts connected each other by studs. The concrete slab is 10mm deep and 800mm wide, with one layer of Q131/131 steel web. The concrete used is C25. The steel beam used is S275 IPE-200. The schematic view of the steel-concrete composite beam is shown in Figure 2.
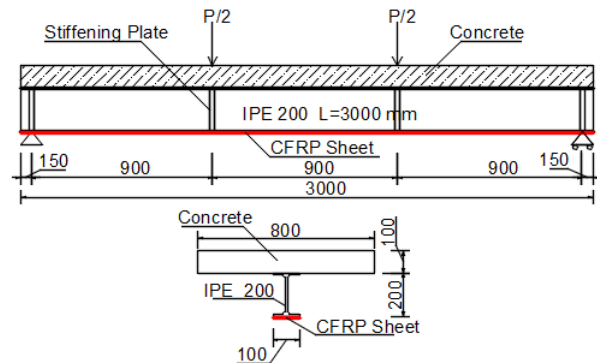

Figure 2. Drawing of test specimen steel-concrete composite Beam

Connection between concrete slab and steel beam was provided by studs. In total, 22 shear steel studs (Figure 3-a) were used. The steel beam with welded studs is shown in Figure 3-b. Stiffening plates (Figure 3-c) were welded to the web of IPE 200 profile from both sides of the web at the support and at the points where the load would be applied.
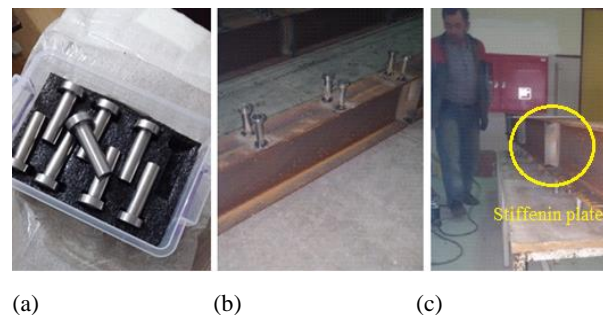

(a)   (b)   (c)

Figure 3. Headed studs and stiffening Plates [15]

100×800×3000 mm concrete molds were prepared (Figure 4-a), welded wire fabric was placed 25 mm deep from surface of the concrete slab. Welded wire fabric

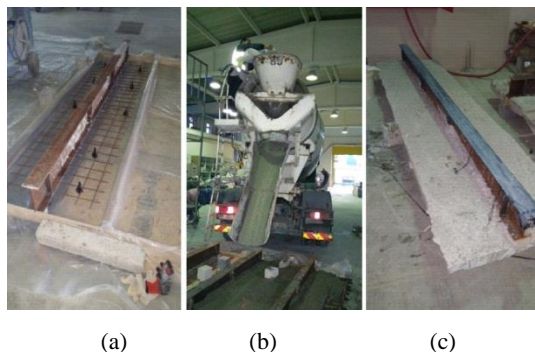type is chosen as Q131/131, and concrete casting was completed by trans-mixer (Figure 4-b and Figure 4-c).

(a)　　　　(b)　　　　(c)

Figure 4. Mold, concrete casting and CFRP strengthened steel-concrete composite beam.

In experimental study, three types of steel-concrete composite beams prepared and have been tested. One of the samples is considered as control sample that is simple steel-concrete composite beam without retrofitting (CBWOCFRP). The other two are steel-concrete composite beams strengthened with two layers of CFRP sheets at lower flange of I shaped steel profile (CBW2CFRP) and strengthened with three layers of CFRP sheets at lower flange of I shaped steel profile (CBW3CFRP). The samples were tested for 4-point bending test under cyclic load. CFRP sheets are bonded to the lower flange of the IPE 200 (Figure 4-c). The strengthening procedure includes removing rust from steel with sand blasting, and cleaning by acetone to ensure good and strong bonding. CFRP sheets were bonded by applying priming adhesive layer Sikadur 330 then by applying SikaWrap 300C. In order to avoid air pockets or irregularities, sheets were located onto the epoxy coating and were pressed diligently. This process was continued until the resin was squeezed out between the roving of the fabric. It should be noted that additional epoxy resin was spread on after applying the previous layer. The application implemented two layers for specimen CBW2CFRP and three layers for CBW3CFRP specimens. CFRP applications were carried out at room temperature and all specimens were cured for at least 28 days before testing.

2.1. Mechanical Properties of Concrete

The C25 concrete mixtures were prepared in the factory and brought to the laboratory by a trans-mixer. Cube and cylindrical samples were taken while concrete casting and tested on the same day with steel-composite beams were tested. Compressive strength of concrete was determined by uni-axial compression tests on 150 mm dimensional cube samples according to TS EN 12390-3 standard. The rate of loading was set as 6.8 kN/s. Tensile strength of the concrete was determined by splitting tensile strength test on cylindrical samples with 100 mm diameter and 200 mm height according to TS EN 12390-6 standard and the rate of loading was set as 3 kN/s. Modulus of elasticity test was carried out on 100 mm

dimensional cube samples. [16,17]. The results of the tests are given in Table 1.

Table 1. Mechanical properties of concrete

Concrete of sample	Uniaxial strength (MPa)	Splitting tensile strength (MPa)	Modulus of Elasticity (MPa)
CBWOCFRP	28.26	2.8	30026
CBW2CFRP	29.3	2.8	29896
CBW3CFRP	29.3	2.8	29996

2.2. Mechanical Properties of CFRP and Steel Beam

Carbon fiber sheets used for strengthening of the steel-concrete composite beam is SikaWrap 300C and bonding resin used is epoxy Sikadur 330. Mechanical properties of CFRP and the epoxy resin are presented in Table 2.

Table 2. Mechanical properties of CFRP

Properties of unidirectional CFRP	Remarks of SikaWrap 300C
Fiber orientation	0°
Areal weight (g/m2)	300±10
Density (g/m3)	1.78x10-6
Thickness (mm)	0.166
Tensile strength (MPa)	3.900
Elastic modulus (MPa)	230.000
Ultimate tensile strain (%)	1.5%

Table 2. Mechanical properties of Epoxy

Properties of resin	Remarks of Sikadur 330
Tensile strength (MPa)	30
Elastic modulus (MPa)	3800
Properties of Lamina (1 mm for each layer)	**Remarks of Sika**
Elastic modulus (GPa)	33

Steel profile used as a part of the steel-concrete composite beam is IPE200 with 275 MPa yielding and 410 MPa ultimate strength capacity steel beam. Elasticity modulus of the steel is 200 GPa. The Yield strain ε_y (mm/mm) and ultimate strain ε_u (mm/mm) values are 1900 $\mu\varepsilon$ and 350000 $\mu\varepsilon$, respectively.

2.3. Experimental Setup

The 3 meter beam was loaded as in Figure 5 in the 4-point loading test. The 500 kN load capacity load cell was used. Deformations were measured by displacement meters and strains were measured by strain gauges. A total of three displacement meters were placed to the l/4 and 1/2 of the beam. Strain-gauges were placed on the upper and lower flanges of the middle of the IPE 200 profile to measure the max strain values. Thus, the yielding was easily identified when it would occur. Location of displacement meters and strain gauges are shown in Figure 5, as well. Load value was obtained with the help of the 500kN load cell. The data that came from all these sensors were transferred to the computer with the Testbox1001 data acquisition system which has a sampling rate 8 S/s. The load and strain values were

transferred to the computer by National Instruments 9237 24bit data acquisition system. The cyclic loading was increased 25 kN in each cycle. Incremental cyclic loading was continued until the failure of the beam.
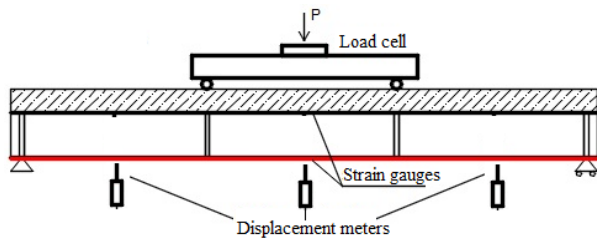

Figure 5. Schematic view of test set-up.

Testing is shown in Figure 6.

Figure 6. Steel-concrete composite beam test set-up

2.4. FEM Model of the Steel-concrete composite beams

FEM model of the steel-concrete composite beam was prepared in the ATENA-GiD program [18] that is a new generation stress analysis program specially designed for concrete, which makes it easier for the user since default values given for concrete are designed considerably well. In addition to that in case of serious cracking occurrence in concrete, in FEM analysis, the convergent is reached. The bonding between concrete and steel beam is constituted via "fixed contact" as explained in ATENA program documentation Part 4-6 [19] to ensure fully steel-concrete composite beam model. The finite element model of the control beam consists of 32958 tetrahedral elements 89 line elements and 9598 nodes (Figure 7). CFRP are assigned as linear elements to the flange of the steel beam as explained in the Atena program documentation part 4-9 and 11 for CFRP strengthened model [19]. The strengthened beam models have 300 additional line elements and 315 nodes that represent CFRP (Figure 8). The material properties of concrete obtained as a result of the tests were added to the program. Material properties given by the manufacturers were used for steel and CFRP material. Displacement values obtained in the experimental results are given as input data for the nonlinear FEM model.
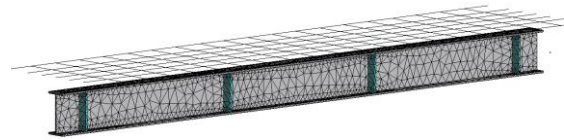

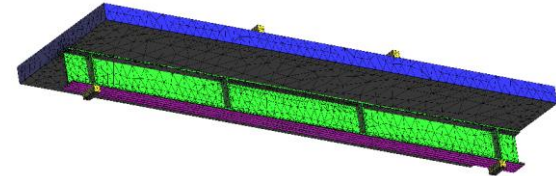**Figure 7.** FEM model of the steel-concrete composite beam

Figure 8. FEM model of the CFRP strengthened steel-concrete composite beam

2.5. Experimental Results and Evaluation
2.5.1. Control sample (CBWOCFRP)

Load-deflection, Strain-time and Load-time graphs of control sample (CBWOCFRP) steel-concrete composite beam are given in Figure 9 and 10. Under cyclic loading, permanent deformations occurred after the 9th load cycle at 225 kN (Figure 9). The first micro shear cracks occurred in the 7th load cycle at 175 kN at the points where the load was impacted. Yielding in the composite beam was observed at the 325 kN load and after that deflections increased (Figure 10 and 11) and shear cracks expanded rapidly in the region near the area of the load implementation of concrete slab (Figure 12). Brittle fracture in steel-concrete composite beam was not observed until the failure of the system.
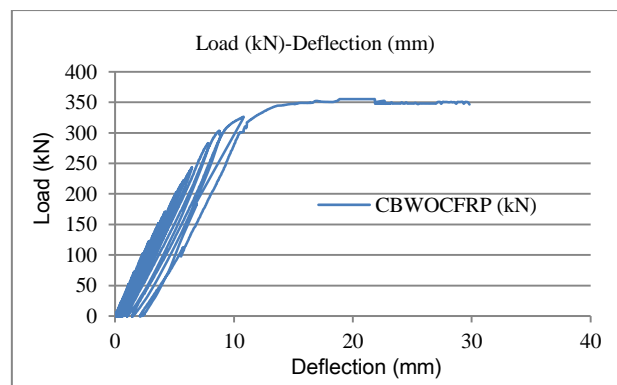

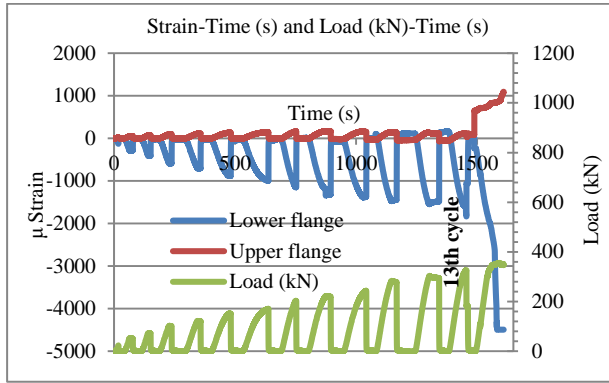**Figure 9.** Incremental cyclic load-deflection graph of CBW0CFRP sample

Figure 10 Strain-time and Load-time graphs of CBW0CFRP sample

Figure 11. Deformed shape of the CWOCFRP sample

Figure 12. Shear cracks of the CWOCFRP sample

2.5.2. Sample strengthened with two layers CFRP (CBW2CFRP)

Load-deflection, Strain-time and Load-time graphs graph of CBW2CFRP steel-concrete composite beam are given in Figure 13 and 14. Permanent deformations occurred after the 10th load cycle at 250 kN and the rigidity of the system and slope of the load-displacement curve began to decrease slowly. Also the bonding between CFRP and steel begin to lose as seen from the Figure 15, at about 10th cycle. In Figure 16 the strain value of lower flange of the steel exceeds 1900 με which is yielding strain value of steel this shows the CFRP cannot prevent the yielding of steel because of insufficient proportion. When the CFRP sheet near the edges begins to rupture, the strain value of the mid CFRP increased. A significant yielding in the system was observed at the 380 kN (Figure 13) load also at this load the CFRP was ruptured with a noise at edges (Figure 15), this was followed by increase in deflection. Shear cracks expanded suddenly in the region near the area of the load implementation and the concrete slab crushed (Figure 16). Brittle fracture in concrete was not observed until the failure of the system. The deformed sample is presented in Figure 17.
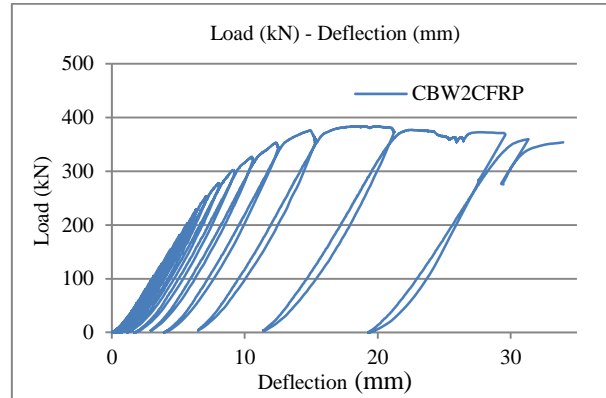

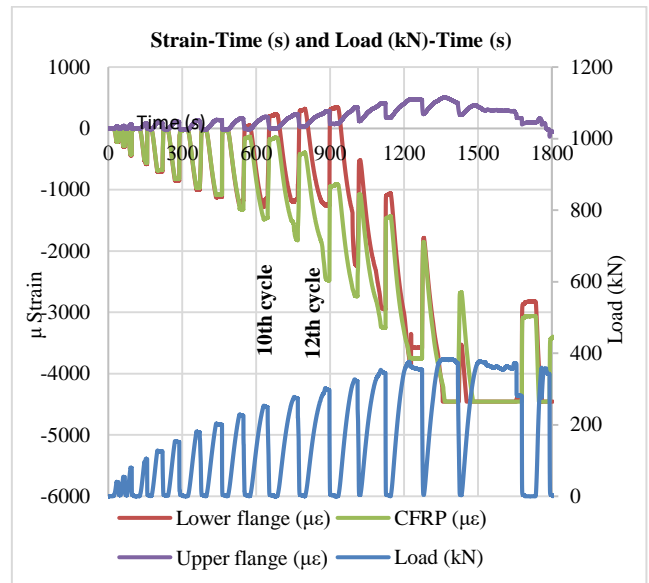**Figure 13.** Incremental cyclic load-deflection graph of CBW2CFRP sample

Figure 14. Strain-time-and Load-time graphs of CBW2CFRP sample

Figure 15. Rupture at edges and de-bonding of CFRP from steel in CBW2CFRP sample

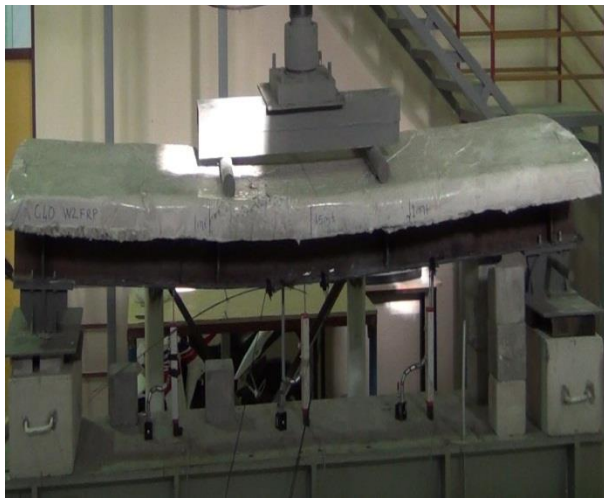**Figure 16.** Shear cracks near the loading point

Figure 17. Deformed shape of the strengthened sample

2.5.3. Sample strengthened with three layers CFRP (CBW3CFRP)

Load-deflection, Strain-time and Load-time graphs graph of CBW3CFRP steel-concrete composite beam are given in Figure 18 and 19. Permanent deformations clearly happened after the 11th load cycle at 275 kN and the rigidity of the system and slope of the load-displacement curve began to decrease. The bonding between CFRP and steel begin to lose at 12th cycle 300kN as seen from the Figure 18. Also the first capillary shear cracks occurred in the points where the load was impacted. From Figure 19 it is seen that the yielding of the steel lower flange was prevented by CFRP and the strain value of the steel was limited although the separation of CFRP from steel is occurred at mid-span. This is because the CFRP is implemented entirely under lower flange and anchored from support points. However after 14th cycle when the load is removed, compression strain is observed on steel flange and tension strain observed on CFRP. This is because after plastic deformation of the system the lower steel flange of the steel-concrete composite beam elongates and because CFRP is not ruptured and still in it is in elastic region it applies tension to the lower steel flange. A significant yield in the beam was observed at the 476 kN. After yielding, the amount of deflection

increased and shear cracks expanded suddenly in the region near the area of the load implementation and the concrete slab crushed (Figure 20). And load carrying capacity of the beam decreased to 350 kN but still can carry load.
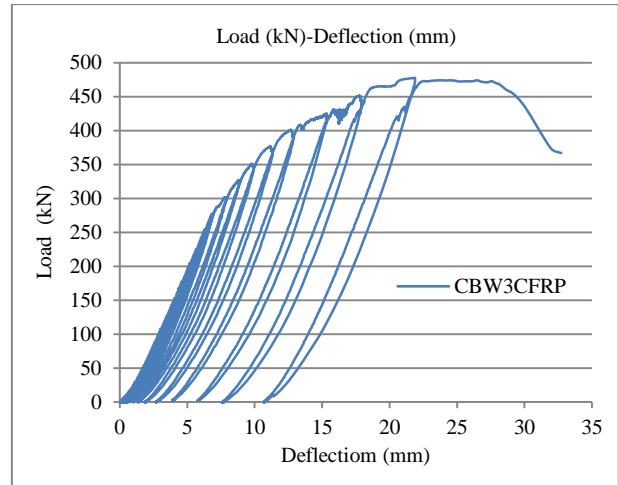

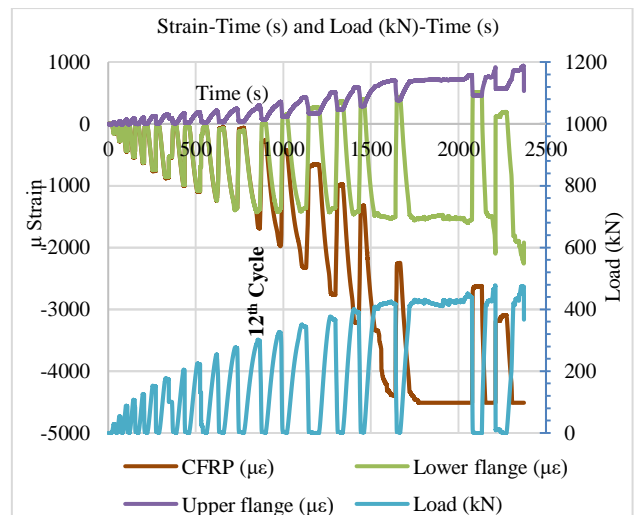**Figure 18.** Incremental cyclic load-deflection graph of CBW3CFRP sample

Figure 19. Strain-time-and Load-time graphs of CBW3CFRP sample

Figure 20. Concrete crushing and deflection of CBW3CFRP sample

All the samples exhibited considerably high ductile behavior, as expected. Failure of the control sample without strengthening was depending failure of concrete

slap. Yielding of the steel beam fallowed by concrete crash was occurred, because the steel beam did not have strength to reverse the deformation in concrete slap. On the other hand, yielding capacity was increased due to CFRP, although the concrete slap was crashed, steel beam had capacity reverse the deformation, and exhibited larger load carrying capacity and ductility.

3. FINITE ELEMENT ANALYSIS OF THE STEEL-CONCRETE COMPOSITE BEAM

The finite element models for the steel-concrete composite beam given in Section 2.4 were analyzed. The maximum deflection-total load value graph was obtained from the analyses and is presented in Figure 21 for three models. The crack map and principle stress contour graphs obtained for non-strengthened and strengthened steel-concrete composite beams and the stress distribution are given in Figures 22, 23 and 24.
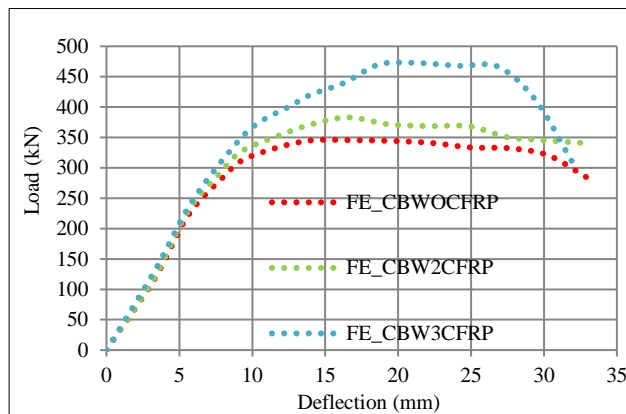

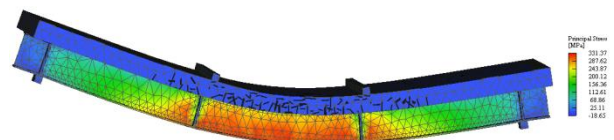**Figure 21.** Load-deflection curves obtained from ATENA-GID FEM program

Figure 22. Principle stress contour and cracks in un-strengthened steel-concrete composite beam (CBW0CFRP)
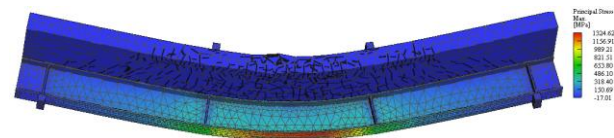

Figure 23. Principle stress contour and cracks in strengthened with two layers of CFRP steel-concrete composite beam (CBW2CFRP)
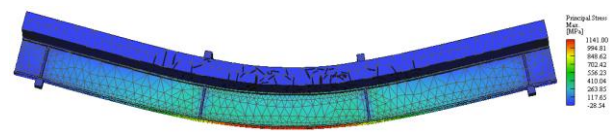
Figure 24. Principle stress contour and cracks in strengthened with three layers of CFRP steel-concrete composite beam (CBW3CFRP)

4. RESULTS AND DISCUSSION

The comparison of experimental and finite element analysis is given in Figure 25. The linear regions of the load-deflection graphs for experiment and nonlinear FEM analysis are overlapped. The maximum load of the experimental and FEM analysis results are similar. The reason for increase in rigidity is that the modulus of elasticity of CFRP is 230 GPa and of steel is 200 GPa. The bonding between steel beam and CFRP sheet was provided well, so that these two materials worked together, result in increase in load carrying capacity of the steel-concrete composite beam. A detailed comparison of the results is presented in Table 3 and Table 4.

The CFRP sheets bonded entirely on lower flange and anchored at support points if this was not implemented the CFRP will de-bonded entirely from the steel due to yielding of steel. Nonlinear FEM model and experimental results show good agreement. Bonding the CFRP sheets entirely to the steel flange has an advanced not to fail although de-bonding occurs and the system carry the load. But this time concrete crushing occurred so the compressive strength of the concrete must also be increased. If CFRP is used for strengthening in composite structures concrete must also strengthened by increasing slab height.
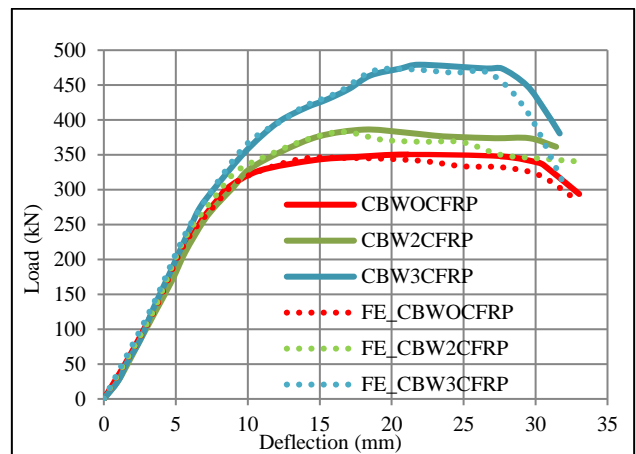

Figure 25. Load-deflection curves obtained from numerical model and experimental study

Table 3. Comparison of experimental results

Property	CB WOCFRP	CB W2CFRP	CB W3CFRP
First Crack Load (kN)	175	200	200
First permanent deformation load (kN)	225	250	275
Yielding Load (kN)	325	380	470

Maximum Load	350	383	474
Increase ratio of maximum load (%)	-	9.4	35.4
Failure Type	yielding	yielding	yielding

Table 4. Comparison of FEM results

Property	FEM CB WOCFRP	FEM CB W2CFRP	FEM CB W3CFRP
First Crack Load (kN)	180	190	190
Yielding Load (kN)	375	380	470
Maximum Load (kN)	350	380	470
Increase ratio of maximum load (%)	-	8.5	34
Failure Type	yielding	yielding	yielding

5. CONCLUSIONS AND RECOMMENDATIONS

Flexural capacity of the steel-concrete composite beams is controlled by bottom flange of the steel section and concrete slab. Increasing tension force capacity in where the tension is effected provides better flexural strength. In this study, tension region of steel-concrete composite beam (bottom flange of steel beam) is strengthened using carbon fiber reinforced polymer (CFRP) sheet in order to have better flexural behavior. Both the steel-concrete composite beam and CFRP strengthened steel-concrete composite beam are analyzed both analytically and experimentally. Results of the analyses exhibited that the reasonable increase in flexural behavior capacity is possible if certain amount of CFRP applied. According to results of experimental and numerical studies, following conclusions and recommendations are made.

Experimental and numerical results of the steel-concrete composite beams have given the similar flexural stiffness in the linear region of load-displacement curve, because the elasticity modulus of steel and CFRP are close to each other, and cross section proportion of CFRP is small according to steel.

Although CFRP have a small effect on stiffness, load carrying capacity of the beams increased 8.5 % and 34 % for CBW2CFRP and CBW3CFRP samples, respectively. Increasing the number of layers of CFRP will increase the maximum load. Hence, shear strength of the beam which is compensated by web of the steel beam should be taken into account.

Regarding failure modes, flexural capacity and failure of the beam are controlled by CFRP. The failure occurred after yielding of the steel beam, delamination between steel bottom flange and CFRP, rupturing of the CFRP and concrete crushing, respectively. On the other hand, because of existence of the structural steel beam, even after concrete crushed, the beam still has capacity to carry load. Because of high proportion of CFRP in CBW3CFRP sample and by providing very good CFRP/steel bonding at the support region, the tension stresses transferred to the steel beam from CFRP completely in the middle section of the beam.

For FEM modeling, embedding CFRP as linear elements into the steel simulates maximum loading capacity very well, however, delamination cannot be seen. For this reason, if there is no delamination this is a good solution for CFRP FEM modeling.

ACKNOWLEDGEMENT

REFERENCES

[1] Arda T.S. and Yardımcı N., "*Çelik Yapıda Karma Elemanların Plastik Hesabı*", Birsen Yayınevi, İstanbul, (2000).

[2] "*Çelik Yapıların Tasarım ve Yapım Kuralları*", Çevre ve Şehircilik Bakanlığı, Ankara, (2016).

[3] Price A.M. and Anderson D., "Const steel design Part 4", Composite beams, *Elsevier Applied Science*, (1992).

[4] Tavakkolizadeh M. and Saadatmanesh H., "Strengthening of steel-concrete composite girders using carbon fiber reinforced polymers sheets", *Journal of Structural Engineering*, *ASCE* 129(1): 30-40, (2003).

[5] Fam A., MacDougall C. and Shaat A., "Upgrading steel-concrete composite girders and repair of damaged steel beams using bonded CFRP laminates", *Thin-Walled Structures*, 47(10): 1122-1135, (2009).

[6] Al-Saidy A.H., Klaiber F.W., Wipf T.J., AI-Jabri K.S. and AI-Nuaimi, A.S., "Parametric study on the behavior of short span composite bridge girders strengthened with carbon fiber reinforced polymer plates", *Construction and Building Materials*, 22:729-737, (2008).

[7] Rizkalla S., Dawood M. and Schnerch D., "Development of a carbon fiber reinforced polymer system for strengthening steel structures", *Composites Part A: Applied Science and Manufacturing*, 39(2): 388-397, (2008).

[8] Seleem M.H., Sharaky I.A. and Sallam H.E.M., "Flexural behavior of steel beams strengthened by carbon fiber reinforced polymer plates three dimensional finite element simulation", *Materials & Design*, 31(3): 1317-24, (2010).

[9] Teng J. G., Fernando D. and Yu T., "Finite element modeling of bonding failures in steel beams flexural strengthened with CFRP laminates", *Engineering Structures*, 86: 213-224, (2015).

[10] El-Shihy A.M., Fawzy H.M., Mustafa S.A. and El-Zohairy A.A., "Experimental and numerical analysis of composite beams strengthened by CFRP laminates in hogging moment region", *Steel and Composite Structures*, 10(3): 281-295, (2010).

[11] Pecce M., Rossi F., Bibbò F.A. and Ceron F., "Experimental behavior of composite beams subjected to a hogging moment", *Steel and Composite Structures*, 12(5): 395-412 395, (2012).

[12] Lin W., Yoda T.and Taniguchi N., "Fatigue tests on straight steel–concrete composite beams subjected to hogging moment", *Journal of Constructional Steel Research*, 80: 42–56, (2013).

[13] Değerli A., "Bulonlar ile birleştirilmiş kompozit kirişlerin negatif moment bölgesindeki yapısal davranışları",

Master's Thesis, Sakarya University, Institute of Science and Technology, (2012).

[14] Ağcakoca E., and Aktaş M., "HM-CFRP ile güçlendirilmiş kompozit I-kirişlerde HM-CFRP'nin sıyrılmaması için faydalı mesafenin belirlenmesi", *E-Journal of New World Sciences Academy*, 7(2): 47-59, (2012).

[15] Özyılmaz E.," Karbon Lifler İle Güçlendirilmiş Kompozit Kirişlerin Eğilme Ve Kesme Kuvveti Altında Davranışlarının Deneysel Olarak İncelenmesi", *Master's Thesis*, Ege University, Institute of Science and Technology, (2016).

[16] Erdoğan T.Y., "*Beton*", Middle East Technican University Publishing*,* Ankara, Türkiye, (2013).

[17] TS 500, "*Betonarme Yapıların Tasarım ve Yapım Kuralları*, (2000).

[18] ATENA version 5.3, Červenka Consulting s.r.o., Prague, Czech Republic, 2016.

[19] Pryl D., and Červenka J., ATENA Program Documentation, Červenka Consulting s.r.o., Prague, Czech Republic, 2016.